

SiGe quantum dots for fast hole spin Rabi oscillations

N. Ares,[†] G. Katsaros,^{*,†,‡,¶} V. N. Golovach,^{‡,§,||} J. J. Zhang,[‡] A. Prager,[†]
L. I. Glazman,[⊥] O. G. Schmidt,^{‡,#} and S. De Franceschi^{*,†}

SPSMS/LaTEQS, CEA-INAC/UJF-Grenoble 1, 17 Rue des Martyrs, 38054 Grenoble Cedex 9, France, Institute for Integrative Nanosciences, IFW Dresden, Helmholtzstr. 20, D-01069 Dresden, Germany, Johannes Kepler University, Institute of Semiconductor and Solid State Physics, Altenbergerstr. 69, 4040 Linz, Austria, Centro de Física de Materiales CFM/MPC (CSIC-UPV/EHU) and Donostia International Physics Center DIPC, E-20018 San Sebastián, Spain, IKERBASQUE, Basque Foundation for Science, E-48011 Bilbao, Spain, Department of Physics, Yale University, New Haven, Connecticut 06520, USA, and Center for Advancing Electronics Dresden, TU Dresden, Germany

E-mail: georgios.katsaros@jku.at; silvano.defranceschi@cea.fr

Abstract

We report on hole g-factor measurements in three terminal SiGe self-assembled quantum dot devices with a top gate electrode positioned very close to the nanostructure. Measurements

*To whom correspondence should be addressed

[†]SPSMS/LaTEQS, CEA-INAC/UJF-Grenoble 1, 17 Rue des Martyrs, 38054 Grenoble Cedex 9, France

[‡]Institute for Integrative Nanosciences, IFW Dresden, Helmholtzstr. 20, D-01069 Dresden, Germany

[¶]Johannes Kepler University, Institute of Semiconductor and Solid State Physics, Altenbergerstr. 69, 4040 Linz, Austria

[§]Centro de Física de Materiales CFM/MPC (CSIC-UPV/EHU) and Donostia International Physics Center DIPC, E-20018 San Sebastián, Spain

^{||}IKERBASQUE, Basque Foundation for Science, E-48011 Bilbao, Spain

[⊥]Department of Physics, Yale University, New Haven, Connecticut 06520, USA

[#]Center for Advancing Electronics Dresden, TU Dresden, Germany

of both the perpendicular as well as the parallel g-factor reveal significant changes for a small modulation of the top gate voltage. From the observed modulations we estimate that, for realistic experimental conditions, hole spins can be electrically manipulated with Rabi frequencies in the order of 100MHz. This work emphasises the potential of hole-based nano-devices for efficient spin manipulation by means of the g-tensor modulation technique.

Keywords: nanoelectronics, silicon, germanium, Rabi oscillation, g-factor.

Important progress has been made in the past years in the coherent manipulation of confined spins in semiconductor quantum dots (QDs) by means of oscillating magnetic and electric fields.^{1,2} Spin states can be electrically manipulated either by electric-dipole spin resonance (EDSR)³⁻⁵ or by the so-called g-tensor modulation technique.^{6,7}

The EDSR technique is based on the fact that the ac electric field shifts the orbital wavefunction back and forth; in an external static magnetic field, due to the presence of a strong spin-orbit coupling, this oscillatory motion induces coherent spin rotations. On the other hand, in the g-tensor modulation technique, spin rotations result from an electrically induced oscillation of the Zeeman vector. Electrically tunable g-factors are thus essential for this technique.

In the past decade, g-factors in different QD systems have been studied thoroughly.⁸⁻¹⁴ Recently, Deacon et al.⁸ reported electrically tunable electron g-factors for self-assembled InAs nanocrystals (NCs) and estimated the electron Rabi frequency for their double-gate geometry. Since the gates were positioned rather far from the NCs, however, the resulting Rabi frequencies were estimated to be only around 2MHz.

Interestingly, holes had not been considered as potential qubits for a long time, since their spin relaxation times were expected to be very short due to the strong spin-orbit (SO) interaction. In spite of the presence of hyperfine interaction and SO coupling, however, experiments with InGaAs QDs have shown spin relaxation times, T_1 , as high as several hundreds of microseconds.¹⁵ Since in the absence of hyperfine interaction¹⁶ the spin decoherence time, T_2 , is predicted to be equal to $2T_1$, hole-confinement QDs based on isotopically purified SiGe nanostructures are promising candidates for spin qubits with long coherence time.

Hole-confinement QDs have been realized in Ge/Si core/shell nanowires,^{17,18} where hole spin relaxation times in the order of 1ms were recently reported.¹⁹ In order to realize hole-based spin qubits in these systems, the development of all-electrical efficient techniques for fast spin rotations is essential,²⁰ because time-dependent magnetic fields are inefficient at inducing Rabi oscillations for holes.²¹

In this work we have studied holes confined in SiGe NCs. We have placed a top gate 6 – 7 nm away from the NCs, which allows us to electrically tune the g-factor of the hole state. Placing a top gate so close to the NC has several advantages. Firstly, as the coupling to the QD is very strong, driving of the spin states with Rabi frequencies of the order of 100MHz can be achieved. In addition, as the gate can be very narrow, its action is local and the dissipation of the high-frequency power is minimized.

The SiGe self-assembled NCs used in this study were grown on undoped (n-) Si(001) wafers. The NCs were contacted by aluminium leads [see Fig.1(A)] and the top gates were created by depositing 6nm of hafnia on top of the obtained devices, followed by deposition of a Ti/Pt 10/90nm metal electrodes. Low-temperature transport measurements were carried out in a dilution refrigerator with a base temperature of 15 mK equipped with accurately filtered wiring and low-noise electronics. A typical differential conductance (dI_{sd}/dV_{sd}) measurement as a function of the top-gate (V_{tg}) and source-drain (V_{sd}) voltages is shown in Fig. 1 (B). A small magnetic field, $B = 70$ mT, is applied in order to suppress the superconductivity of the Al electrodes.

Diamond-shaped regions with a charging energy of about 2 meV can be observed in Fig. 1 (B). In the Coulomb blockade regime, single-hole transport is suppressed and electrical conduction is due to second-order cotunneling (CT) processes.²² Each CT process involves a hole tunneling out of the QD into the right contact and, simultaneously, another hole entering the QD from the left contact. At small V_{sd} , CT is said to be elastic since it cannot create any excitation in the QD. At sufficiently large V_{sd} , however, CT processes can leave the QD in an excited state. Such processes are thus referred to as inelastic. Both diamonds shown here show such inelastic CT features, visible as steps in the dI_{sd}/dV_{sd} . From the position of the inelastic CT step we conclude that the orbital

level separation for this device is about $200 \mu\text{eV}$.

In order to determine the even or odd occupation of each diamond we performed CT spectroscopy measurements as a function of an applied magnetic field, B . These measurements are shown in Fig. 1 (C)-(D), for the left and right diamond, respectively. A clearly different behavior is observed, revealing the distinct character of the ground states in the two adjacent diamonds. These different behavior of the CT steps as a function of B , already reported in ¹³ is attributed to a left (right) diamond correspondent to an odd (even) number of charges.

The differential conductance of the odd diamond was studied further in order to gain more insight into the Zeeman-split Kramers. Figs. 2 (A) and 2 (B) show a stability diagram of this diamond for $B = 0.6$ T applied perpendicular and parallel to the growth plane, respectively. Steps due to the presence of inelastic CT processes are again observed.

By fixing V_{tg} within the Coulomb blockade regime and sweeping the magnetic field, the behavior of the CT steps was investigated. These measurements are shown in Figs. 2 (C)-(D). As the CT steps merge together when B approaches zero, we can confirm that the observed steps correspond to the Zeeman splitting of the ground state (E_Z). The g -factor value perpendicular (g_{\perp}) and parallel (g_{\parallel}) to the substrate plane can be extracted from these measurements since $E_Z = g\mu_B B$, with μ_B being the Bohr magneton. The extracted values are $g_{\perp} = (2.0 \pm 0.2)$ and $g_{\parallel} = (1.2 \pm 0.2)$.

Let us now remark on the fact that in both diamonds in Figs. 2 (A)-(B), the inelastic CT steps are not parallel to the V_{tg} axis. This slope in the CT steps demonstrates that both g -factors values are voltage and thus electric-field dependent. From the reported measurements we extract $\frac{\partial g_{\parallel}}{\partial V_{tg}} = (0.008 \pm 0.001) \frac{1}{mV}$ and $\frac{\partial g_{\perp}}{\partial V_{tg}} = (0.007 \pm 0.001) \frac{1}{mV}$.

In order to estimate the Rabi frequency, we consider an oscillating voltage V_{ac} superimposed to a constant value V_{tg} . Provided that V_{ac} is sufficiently small, the dependence of g_{\parallel} and g_{\perp} on V_{tg} can be assumed to be linear and the Rabi frequency of the induced spin rotations reads (see Supporting Information)

$$f_R = \frac{\mu_B V_{ac}}{2h} \left[\frac{1}{g_{\parallel}} \left(\frac{\partial g_{\parallel}}{\partial V_{tg}} \right) - \frac{1}{g_{\perp}} \left(\frac{\partial g_{\perp}}{\partial V_{tg}} \right) \right] \times \frac{g_{\parallel} g_{\perp} B_{\parallel} B_{\perp}}{\sqrt{(g_{\parallel} B_{\parallel})^2 + (g_{\perp} B_{\perp})^2}}, \quad (1)$$

where h is the Planck constant. In this expression, $B_{\parallel} = B \cos \theta$ and $B_{\perp} = B \sin \theta$, where the angle θ is measured with respect to the growth plane. Further, it can be shown that f_R is maximal if θ is chosen such that

$$\theta_{max} = \arctan \sqrt{\frac{g_{\parallel}}{g_{\perp}}}. \quad (2)$$

The experimental values obtained for g_{\parallel} , g_{\perp} , $\frac{\partial g_{\parallel}}{\partial V_{tg}}$ and $\frac{\partial g_{\perp}}{\partial V_{tg}}$, were used to estimate f_R for a given value of the Larmor frequency (f_L) and for different values of θ (see Fig. 3).

By considering a driving frequency $f_L \approx 20$ GHz, which corresponds to $B \approx 0.9$ T applied at an angle θ_{max} , we obtain a Rabi frequency $f_R \sim 100$ MHz for $V_{ac} \approx 7$ mV. Taking the lever-arm parameter of the gate electrode,²³ $\alpha \approx 0.07$, this value of V_{ac} corresponds to an energy shift of $\approx 500 \mu eV$, which is of the same order of typically energy-level modulations in EDSR experiments.^{5,24} We note that the estimated value for the Rabi frequency is comparable to values recently reported for electrons confined in InSb nanowires.²⁴

In summary, we have demonstrated that a single top-gate electrode, defined close to a SiGe self-assembled QD, may enable us to perform spin manipulations by means of the g-tensor modulation technique. Our measurements demonstrate that fast Rabi frequencies can be achieved for realistic experimental conditions. The obtained values together with the expectedly long spin coherence times for carriers in Ge underline the potential of holes confined in SiGe QDs as fast spin qubits.

Supporting Information Available

In order to derive the expression for the Rabi frequency in the main text, let us consider a spin 1/2 driven by the g-tensor modulation. The time evolution of the spin is governed by the Bloch

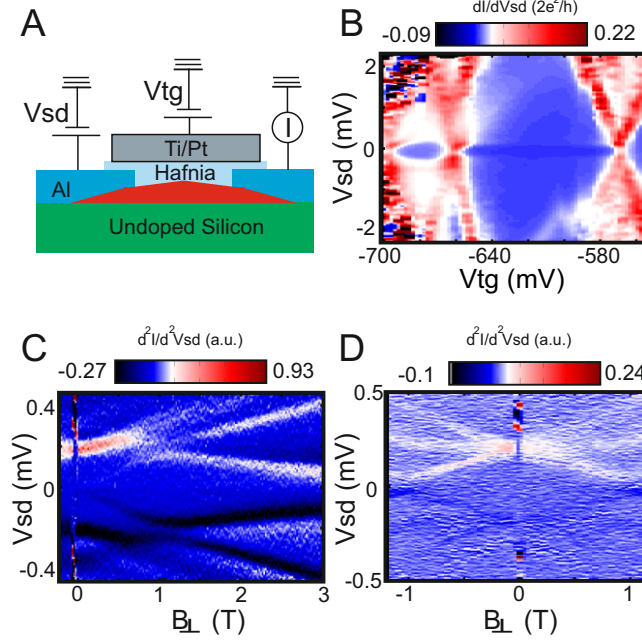


Figure 1: (A) Schematic of a SiGe self-assembled QD device. (B) dI_{sd}/dV_{sd} vs V_{tg} and V_{sd} for $B = 70mT$. The magnetic field is needed for suppressing the superconductivity of the Al electrodes. Inelastic CT steps originating from different orbital levels are present in both diamonds. (C)-(D) numerical derivative d^2I_{sd}/d^2V_{sd} vs. V_{sd} and B_{\perp} for the left and right diamond, respectively. In (C) transitions between two splitted Kramer levels are observed, indicating thus an odd number of localized holes. Transitions between singlet and triplet states are present in (D), implying an even number of confined holes.¹³

equation,

$$\frac{d}{dt} \langle \mathbf{S} \rangle = [\boldsymbol{\omega}_L + \delta \boldsymbol{\omega}(t)] \times \langle \mathbf{S} \rangle, \quad (3)$$

where $\langle \mathbf{S} \rangle$ is the expectation value of the spin $\mathbf{S} = (1/2) \boldsymbol{\sigma}$, with $\boldsymbol{\sigma}$ being the Pauli matrices, $\boldsymbol{\omega}_L$ is the Larmor frequency, and $\delta \boldsymbol{\omega}(t)$ is the time-dependent frequency part due to the driving field. In the g-tensor modulation, the driving field arises because of the ac signal sent to the top gate,

$$V_{tg}(t) = V_{tg}^0 + V_{ac} \sin(\omega_{ac} t), \quad (4)$$

where V_{tg}^0 is the average value of the top-gate voltage, V_{ac} is the resulting amplitude of voltage oscillations, and ω_{ac} is the ac angular frequency. Since we use dome-like SiGe nanocrystals, which roughly obey rotational symmetry about the axis $z \equiv [001]$, the g-tensor \hat{g} is approximately

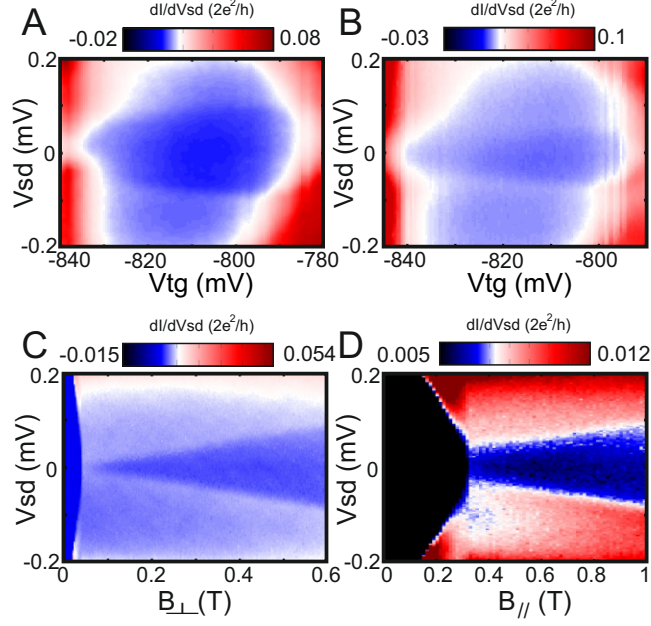


Figure 2: (A)-(B) dI_{sd}/dV_{sd} vs. V_{tg} and V_{sd} for $B = 0.6T$, applied perpendicular and parallel to the substrate plane, respectively. (C)-(D) dI_{sd}/dV_{sd} vs. B and V_{sd} for perpendicular and parallel magnetic fields, respectively, demonstrating that the inelastic CT steps are due to the Zeeman splitting of a spin $\frac{1}{2}$ ground state. From the measured Zeeman energies we estimate $g_{\perp} = (2.0 \pm 0.2)$ and $g_{\parallel} = (1.2 \pm 0.2)$.

diagonal in the main crystallographic frame (x, y, z) . The non-zero elements of \hat{g} include two equal-to-each-other inplane components, $g_x = g_y \equiv g_{\parallel}$, and one out-of-plane component, $g_z \equiv g_{\perp}$. The g-tensor modulation can, therefore, be written as

$$\begin{aligned}
 g_{\parallel}(t) &\approx g_{\parallel}^0 + \alpha_{\parallel} V_{ac} \sin(\omega_{ac} t), \\
 g_{\perp}(t) &\approx g_{\perp}^0 + \alpha_{\perp} V_{ac} \sin(\omega_{ac} t),
 \end{aligned}
 \tag{5}$$

where $g_{\parallel}^0 \equiv g_{\parallel}$ and $g_{\perp}^0 \equiv g_{\perp}$ are constant, $\alpha_{\parallel} = \frac{\partial g_{\parallel}}{\partial V_{tg}}$, and $\alpha_{\perp} = \frac{\partial g_{\perp}}{\partial V_{tg}}$. Here, it was assumed that V_{ac} is sufficiently small, so that g_{\parallel} and g_{\perp} depend linearly on V_{tg} in the voltage window $V_{tg}^0 \pm V_{ac}$. Thus, the Larmor frequency entering in Eq. (??) is identified as

$$\omega_L = \frac{\mu_B}{\hbar} \hat{g} \cdot \mathbf{B},
 \tag{6}$$

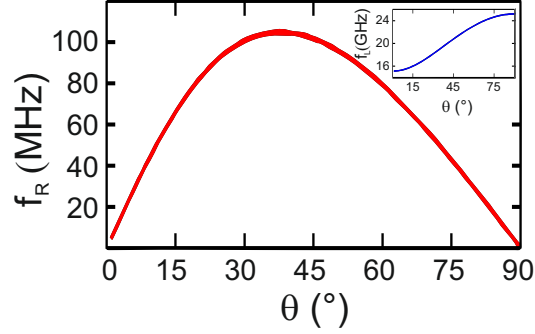


Figure 3: Rabi frequency dependence on the magnetic field angle with respect to the substrate plane (θ). It reaches $\sim 100\text{MHz}$ at $\theta_{max} \approx 38^\circ$. The estimated value corresponds to $B = 0.9T$ and $V_{ac} = 7\text{mV}$. Inset: Larmor frequency as a function of θ for the same experimental conditions. A driving frequency of $\sim 20\text{GHz}$ is estimated for $B = 0.9T$.

whereas the contribution due to driving as

$$\delta \boldsymbol{\omega}(t) = \frac{\mu_B}{\hbar} (\hat{\boldsymbol{\alpha}} \cdot \mathbf{B}) V_{ac} \sin(\omega_{ac} t). \quad (7)$$

To be concise here, we used tensor-vector multiplication, like $(\hat{g} \cdot \mathbf{B})_i = \sum_j g_{ij} B_j$. The tensor of linear coefficients, $\alpha_{ij} = \partial g_{ij} / \partial V_{tg}$, needs not, in general, be proportional to \hat{g} . Therefore, the time-dependent driving $\delta \boldsymbol{\omega}(t)$ may have a component that is transverse to the vector $\boldsymbol{\omega}_L$, *cf.* Eqs. (??) and (??). This circumstance is at the heart of the g -tensor modulation technique used to induce Rabi oscillations.

It is easiest to solve Eq. (??) in a frame rotating at frequency ω_{ac} about the vector $\boldsymbol{\omega}_L$. The time evolution of the spin is approximated as follows

$$\begin{aligned} \langle S_{\pm}(t) \rangle &\approx \tilde{S}_{\pm}(t) e^{\pm i \omega_{ac} t}, \\ \langle S_Z(t) \rangle &\approx \tilde{S}_Z(t), \end{aligned} \quad (8)$$

where $S_{\pm} = S_X \pm i S_Y$ and the coordinate frame (X, Y, Z) has $Z \parallel \boldsymbol{\omega}_L$. The new unknown functions

$\tilde{\mathbf{S}}(t)$ obey a time-independent Bloch equation

$$\frac{d}{dt}\tilde{\mathbf{S}} = (\boldsymbol{\delta} + \boldsymbol{\omega}_R) \times \tilde{\mathbf{S}}, \quad (9)$$

where $\boldsymbol{\delta} = \boldsymbol{\omega}_L(1 - \omega_{ac}/\omega_L)$ is the detuning from resonance and $\boldsymbol{\omega}_R$ is the Rabi frequency given by³

$$\boldsymbol{\omega}_R = \frac{\mu_B V_{ac}}{2\hbar} [(\hat{\boldsymbol{\alpha}} \cdot \mathbf{B}) \times \mathbf{n}], \quad (10)$$

where $\mathbf{n} = \boldsymbol{\omega}_L/\omega_L$ is the unit vector along the Larmor frequency.

Next, we consider the situation realized in the experiment. The magnetic field can be rotated in a plane perpendicular to the substrate. Let us assume that it is the (y, z) -plane and represent the magnetic field as

$$\mathbf{B} = \mathbf{e}_y B_{\parallel} + \mathbf{e}_z B_{\perp}, \quad (11)$$

where \mathbf{e}_i ($i = x, y, z$) are unit vectors. Then, the Rabi frequency reads $\boldsymbol{\omega}_R = \mathbf{e}_x \omega_R$, with

$$\begin{aligned} \omega_R = & \frac{\mu_B V_{ac}}{2\hbar} \left[\frac{1}{g_{\parallel}} \left(\frac{\partial g_{\parallel}}{\partial V_{tg}} \right) - \frac{1}{g_{\perp}} \left(\frac{\partial g_{\perp}}{\partial V_{tg}} \right) \right] \\ & \times \frac{g_{\parallel} g_{\perp} B_{\parallel} B_{\perp}}{\sqrt{(g_{\parallel} B_{\parallel})^2 + (g_{\perp} B_{\perp})^2}}. \end{aligned} \quad (12)$$

In this expression, the two components of the magnetic field are given by $B_{\parallel} = B \cos \theta$ and $B_{\perp} = B \sin \theta$, where θ is the angle of the magnetic field measured with respect to the growth plane. By absolute value, ω_R is largest at

$$\theta = \pm \arctan \left(\sqrt{\left| \frac{g_{\parallel}}{g_{\perp}} \right|} \right), \quad (13)$$

attaining

$$\omega_R = \pm \frac{\mu_B V_{ac}}{2\hbar} \left[\frac{1}{g_{\parallel}} \left(\frac{\partial g_{\parallel}}{\partial V_{tg}} \right) - \frac{1}{g_{\perp}} \left(\frac{\partial g_{\perp}}{\partial V_{tg}} \right) \right] \frac{g_{\parallel} g_{\perp} B}{|g_{\parallel}| + |g_{\perp}|}. \quad (14)$$

Acknowledgement

We acknowledge financial support from the Nanosciences Foundation (Grenoble, France), the Commission for a Marie Curie Career Integration Grant, the Austrian Science Fund (FWF) for a Lise-Meitner Fellowship (M1435-N30), the DOE under Contract No. DE-FG02-08ER46482 (Yale), the European Starting Grant program, and the Agence Nationale de la Recherche. The authors thank J.W.G. van den Berg and S. Nadj-Perge for useful discussions.

References

- (1) Hanson, R.; Kouwenhoven, L.; Petta, J.; Tarucha, S.; Vandersypen, L. *Reviews of Modern Physics* **2007**, *79*, 1217.
- (2) Zwanenburg, F. A.; Dzurak, A. S.; Morello, A.; Simmons, M. Y.; Hollenberg, L. C. L.; Klimeck, G.; Rogge, S.; Coppersmith, S. N.; Eriksson, M. A. *Reviews of Modern Physics* **2013**, *85*, 961–1019.
- (3) Golovach, V. N.; Borhani, M.; Loss, D. *Physical Review B* **2006**, *74*, 165319.
- (4) Nowack, K.; Koppens, F.; Nazarov, Y. V.; Vandersypen, L. *Science* **2007**, *318*, 1430–1433.
- (5) Nadj-Perge, S.; Frolov, S.; Bakkers, E.; Kouwenhoven, L. *Nature* **2010**, *468*, 1084–1087.
- (6) Kato, Y.; Myers, R.; Driscoll, D.; Gossard, A.; Levy, J.; Awschalom, D. *Science* **2003**, *299*, 1201–1204.
- (7) Salis, G.; Kato, Y.; Ensslin, K.; Driscoll, D.; Gossard, A.; Awschalom, D. *Nature* **2001**, *414*, 619–622.
- (8) Deacon, R.; Kanai, Y.; Takahashi, S.; Oiwa, A.; Yoshida, K.; Shibata, K.; Hirakawa, K.; Tokura, Y.; Tarucha, S. *Physical Review B* **2011**, *84*, 041302.
- (9) Csonka, S.; Hofstetter, L.; Freitag, F.; Oberholzer, S.; Schonenberger, C.; Jespersen, T. S.; Aagesen, M.; Nygård, J. *Nano letters* **2008**, *8*, 3932–3935.

- (10) Houel, J.; Prechtel, J. H.; Brunner, D.; Kuklewicz, C. E.; Gerardot, B. D.; Stoltz, N. G.; Petroff, P. M.; Warburton, R. J. *arXiv preprint arXiv:1307.2000* **2013**,
- (11) Roddaro, S.; Fuhrer, A.; Fasth, C.; Samuelson, L.; Xiang, J.; Lieber, C. M. *arXiv preprint arXiv:0706.2883* **2007**,
- (12) Nilsson, H. A.; Caroff, P.; Thelander, C.; Larsson, M.; Wagner, J. B.; Wernersson, L.-E.; Samuelson, L.; Xu, H. *Nano letters* **2009**, *9*, 3151–3156.
- (13) Katsaros, G.; Spathis, P.; Stoffel, M.; Fournel, F.; Mongillo, M.; Bouchiat, V.; Lefloch, F.; Rastelli, A.; Schmidt, O. G.; De Franceschi, S. *Nature nanotechnology* **2010**, *5*, 458–464.
- (14) Ares, N.; Golovach, V.; Katsaros, G.; Stoffel, M.; Fournel, F.; Glazman, L.; Schmidt, O. G.; De Franceschi, S. *Physical Review Letters* **2013**, *110*, 046602.
- (15) Heiss, D.; Schaeck, S.; Huebl, H.; Bichler, M.; Abstreiter, G.; Finley, J.; Bulaev, D.; Loss, D. *Physical Review B* **2007**, *76*, 241306.
- (16) Golovach, V. N.; Khaetskii, A.; Loss, D. *Physical Review Letters* **2004**, *93*, 016601.
- (17) Lu, W.; Xiang, J.; Timko, B. P.; Wu, Y.; Lieber, C. M. *Proceedings of the National Academy of Sciences of the United States of America* **2005**, *102*, 10046–10051.
- (18) Hu, Y.; Churchill, H. O.; Reilly, D. J.; Xiang, J.; Lieber, C. M.; Marcus, C. M. *Nature nanotechnology* **2007**, *2*, 622–625.
- (19) Hu, Y.; Kuemmeth, F.; Lieber, C. M.; Marcus, C. M. *Nature nanotechnology* **2011**, *7*, 47–50.
- (20) Kloeffel, C.; Trif, M.; Stano, P.; Loss, D. *arXiv preprint arXiv:1306.3596* **2013**,
- (21) Sleiter, D.; Brinkman, W. *Physical Review B* **2006**, *74*, 153312.
- (22) De Franceschi, S.; Sasaki, S.; Elzerman, J.; Van Der Wiel, W.; Tarucha, S.; Kouwenhoven, L. P. *Physical Review Letters* **2001**, *86*, 878–881.

(23) The lever arm of a gate electrode is the factor that relates a change of gate voltage to a corresponding shift of the subband energies.

(24) Van den Berg, J.; Nadj-Perge, S.; Pribiag, V.; Plissard, S.; Bakkers, E.; Frolov, S.; Kouwenhoven, L. *Physical Review Letters* **2013**, *110*, 066806.

This material is available free of charge via the Internet at <http://pubs.acs.org/>.